Reynolds stress model assessment using round jet experimental data

William C. Lasher
School of Engineering and Engineering Technology, The Pennsylvania State University at Erie, The Behrend College, Erie, PA, USA

Dale B. Taulbee
Department of Mechanical and Aerospace Engineering, State University of New York at Buffalo, Buffalo, NY, USA

Experimental data of Hussein et al. (1993) for the turbulent round jet are used to evaluate individual components of Reynolds stress turbulence models. Models for terms in the Reynolds stress equations are reviewed, with particular emphasis on linear and nonlinear pressure-strain models. Improved coefficients for the Choi and Lumley return-to-isotropy expressions have been developed by the authors. These coefficients are valid for a wider range of flows than the currently used coefficients. Pressure-strain and transport model components are compared to the experimental data for the jet, and agreement is very good, indicating that the models are reasonably correct. Predictions using the linear models are generally as good as those obtained using nonlinear models, indicating that nonlinear models may not be necessary for engineering accuracy for this flow.

Keywords: Reynolds stress modeling; turbulent jet flow

Introduction

Turbulence models are developed by assuming that the turbulence is in a state where certain simplifying conditions apply. The resulting models are in a strict sense limited by these simplifying conditions, and typically contain one or more coefficients that cannot be determined theoretically. It is therefore necessary to evaluate these models using experimental data, both to validate the underlying assumptions and to determine the coefficients.

The easiest and most common way to evaluate a model is to use a simple flow in which the process of interest is the only process present. For example, in Reynolds stress modeling, the return-to-isotropy term is evaluated using return-to-isotropy experiments, the destruction-of-dissipation term is evaluated using decaying grid turbulence experiments, etc. The disadvantage of this approach is that the process of interest in the simple flow may not be the same as in more complex flows, or the conditions may not be the same as in more complex flows. Taulbee (1987) has shown, for example, that return-to-isotropy models based on return-to-isotropy experiments are inconsistent with several shear flows. This is because the Reynolds number of the turbulence in return-to-isotropy experiments is low compared to the turbulent Reynolds number in these shear flows.

An alternate approach is to use a complete model to simulate a complex flow and to compare the results predicted by the model with experimental results. Individual coefficients in the model can be turned to make the simulation match the experiment. From an engineering viewpoint, this approach has the advantage of allowing the modeler to evaluate the model as a complete package. Deficiencies in one part of the model can be canceled by deficiencies in other parts of the model. While this approach may be necessary and justifiable under some conditions, it can lead to incorrect conclusions about the model, which could result in a misapplication of the model to other flows. In addition, it is difficult for the modeler to pinpoint the weaknesses of the model.

The approach taken in this paper is to find a middle ground between the two approaches just discussed. The round jet provides an opportunity to use a flow in which several physical processes of interest are present, yet individual terms in the modeled equations can still be evaluated. To do so, it is necessary to make some assumptions about the dissipation, which will be discussed later. These assumptions will necessarily affect the resulting comparisons; however, much useful information can still be inferred, and advances in experimental techniques will most likely solve this problem in the future.

A comprehensive set of velocity correlation data for the round jet as developed by Hussein, Capp, and George (1993; 1988; 1983) is used for the present analysis. The experimental results are briefly discussed. The turbulence models of interest in the present work (specifically, Reynolds stress models) are reviewed, including improved expressions for the return-to-isotropy coefficient developed by the authors. The models for the triple-velocity correlation are compared to the data, and the models for the pressure-strain correlation are compared to values obtained by balancing the dynamic equations for the Reynolds stresses. There is good agreement between the models and the data, which suggests that the models are reasonably correct. It is shown that present approach can be used successfully to evaluate turbulence models.

Address reprint requests to Professor Lasher at M-88, Penn State—Behrend, Station Road, Erie, PA 16563-1701.

Received 6 January 1994; accepted 22 May 1994

Summary of experimental results

The experimental data for an axisymmetric jet as presented by Hussein, Capp, and George (1993) are used here. The data were developed using both flying hot wires (HWs) (George and Hussein 1991) and burst-mode laser doppler anemometers (LDAs) (Capp 1983), and include the mean velocity and the second and third moments of the fluctuating velocities. Hussein (1988) also developed stationary HW data that are, as expected, different from the flying HW data and the LDA data. The flying HW data are in general agreement with the LDA data, although the LDA data are in better agreement with a balance of the momentum equation. The LDA data are therefore used for the present analysis; the only missing data in this set are the triple correlation $\overline{vw^2}$ and the spectral measurements for ε. The HW measurements indicate that $\overline{vw^2}$ is approximately equal to $0.55\overline{v^3}$. This approximation will be used in the following analysis.

In order to balance the equations, it is necessary to compute derivatives of each of the variables. To simplify this process, the data for each variable were fit to an equation using least-squares. An appropriate-order polynomial was used to obtain an accurate fit. These equations were then differentiated to obtain expressions for the derivatives.

Dissipation

Direct measurement of the dissipation using stationary probes provides only a rough estimate. The use of Taylor's hypothesis usually is not very accurate if corrections are not made. For this reason, accurate measurements of the dissipation do not exist for this flow (George and Hussein 1991). Different approaches to determining the dissipation produce different and contradictory results, so the exact nature of the dissipation profile must be inferred from physical arguments. In this section, we will discuss several different estimates for the dissipation and explain the basis for selecting a profile.

Hussein (1988) determined the dissipation by balancing the energy equation. All the terms containing only velocity were determined from the LDA data, as described earlier. For lack of something better, the pressure-transport terms were obtained from the closure formula $\overline{pu_i}/\rho = -0.2\overline{u_i q^2}$ given by Lumley (1978). The profile from this balance is shown in Figure 1. Hussein also determined the dissipation from spectral measurements. The spectrum was measured with a hot wire at several positions across the flow and corrected for the effects of fluctuations in the convective velocity (Lumley 1985). The dissipation was computed from the one-dimensional (1-D) energy spectra (Tennekes and Lumley 1972). These results are also shown in Figure 1.

Based on these measurements, one would infer that there is an off-axis peak in the dissipation. The peak from the energy balance is near $\eta = 0.05$, while the spectral measurements indicate a smaller peak near $\eta = 0.03$. The existence of this peak seems reasonable, since the maximum production is not at the centerline; however, one must be careful with these data. The energy balance is uncertain, since there was a fair degree of scatter in the LDA data near the centerline; the profile for $\overline{vw^2}$ was based on HW data; and Lumley's closure formula was used for the pressure transport. The spectral measurements are also uncertain, since HW data were used and more data points need to be taken.

The dissipation was also calculated from the modeled dissipation equation:

$$U\frac{\partial\varepsilon}{\partial x} + V\frac{\partial\varepsilon}{\partial r} = \frac{1}{r}\frac{\partial}{\partial r}\left(r\frac{\nu_t}{\sigma_\varepsilon}\frac{\partial\varepsilon}{\partial r}\right) + (C_{\varepsilon_1}P - C_{\varepsilon_2}\varepsilon)\frac{\varepsilon}{k} \tag{1}$$

where in the standard $k-\varepsilon$ model (Launder et al. 1973), $\nu_t = 0.09k^2/\varepsilon$, $C_{\varepsilon_1} = 1.44$, $C_{\varepsilon_2} = 1.92$, $\sigma_\varepsilon = 1.3$

P in Equation 1 is the turbulent production, and is defined as

Notation

b_{ij}	Anisotropy tensor, $\overline{u_iu_j}/2k - \delta_{ij}/3$
b^2_{ij}	$b_{ik}b_{kj}$
C_1	Linear return-to-isotropy coefficient
C_2	Linear rapid coefficient
C_{2f}	Nonlinear rapid coefficient
$C_{\varepsilon_1}, C_{\varepsilon_3}$	Generation of dissipation coefficients
C_{ε_2}	Destruction of dissipation coefficient
C_s	Stress transport coefficient
D_{ij}	$-(\overline{u_iu_k}\partial U_k/\partial x_j + \overline{u_ju_k}\partial U_k/\partial x_i)$
F	$= 1 + 27\,\mathrm{III} + 9\,\mathrm{II}$
G	Turbulent trajectory function, $-X^4 + 0.8X^6$
G_{ijk}	$\overline{u_iu_l}\dfrac{\partial\overline{u_ju_k}}{\partial x_l} + \overline{u_ju_l}\dfrac{\partial\overline{u_iu_k}}{\partial x_l} + \overline{u_ku_l}\dfrac{\partial\overline{u_iu_j}}{\partial x_l}$
II	Second invariant, $-b_{ik}b_{ki}/2$
III	Third invariant, $b_{ij}b_{jk}b_{ki}/3$
k	Turbulent kinetic energy, $\overline{u_iu_i}/2$
p	Fluctuating pressure
P	Production rate of turbulent kinetic energy, $P_{ii}/2$
P_{ij}	Generation rate of Reynolds stress tensor, $-(\overline{u_iu_k}\partial U_j/\partial x_k + \overline{u_ju_k}\partial U_i/\partial x_k)$
q^2	Turbulent energy, $2k$
r	Jet radius
R_t	Turbulent Reynolds number, $4k^2/9\nu\varepsilon$
S_{ij}	Mean rate of strain tensor, $1/2(\partial U_i/\partial x_j + \partial U_j/\partial x_i)$
t	Time
u, v, w	x, r, θ components of fluctuating velocity
u_i	x_i component of fluctuating velocity
U, V	x, r components of mean velocity
U_c	Jet centerline mean velocity in x-direction
U_i	x_i component of mean velocity
W_{ij}	Mean vorticity tensor, $1/2(\partial U_i/\partial x_j - \partial U_j/\partial x_i)$
x	Distance downstream from virtual jet origin
x_i	Cartesian coordinate
X	ζ/η

Greek symbols

δ_{ij}	Kronecker delta
ε	Dissipation rate of k
γ	Nonlinear return-to-isotropy coefficient
ϕ_{ij}	Pressure-strain correlation
$\phi_{ij,1}$	Return-to-isotropy model
$\phi_{ij,2}$	Rapid model
ρ	Density
ρ^*	Modified characteristic time scale ratio
σ_e	Dissipation transport coefficient
ν	Kinematic viscosity
ν_t	Turbulent viscosity
η	Similarity coordinate, r/x
η	Invariant coordinate, $(-\mathrm{II}/3)^{1/2}$ (Equation 5)
ζ	Invariant coordinate, $(\mathrm{III}/2)^{1/3}$

Subscripts

i, j, k	Cartesian tensor notation

Special Symbols

——	Ensemble average

$-(\overline{u_i u_k})\partial U_i/\partial x_k$. The above equation in similarity form was solved for the dissipation (with all other quantities given by LDA measurement), and the profile is shown as the model profile in Figure 1. Hanjalic and Launder (1980) and Pope (1977) argue that there should be enhanced scale reduction that increases the production of vorticity, and they added a corrective term. Pope's corrective term, $0.25C_{\varepsilon_3}(k^2/\varepsilon)(\partial U/\partial r - \partial V/\partial x)^2 V/R$ (where $C_{\varepsilon_3} = 0.79$), is added to the right side of Equation 1, and the solution is shown in Figure 1 as the corrected model. It is seen that both model results are in good agreement with the LDA balance, except near the centerline, although the corrected model is in better agreement. Neither model predicts the pronounced off-axis peak observed in the LDA balance and spectral measurements.

To see if a model dissipation equation could be developed to produce an off-axis peak, the terms in the basic dissipation equation that are usually neglected were examined. The obvious term to produce such an effect is the term involving the second derivative of the mean flow. Since the curvature of the velocity profile is large near the centerline, this term could significantly affect the dissipation. Unfortunately, this term has the wrong sign and would tend to increase rather than decrease the dissipation in the centerline region. If there is a significant off-axis peak in the dissipation profile, then presumably something is missing in the dissipation equation model.

The off-axis peak has not been observed before either in measurements or in modeling predictions. Other researchers have obtained significantly higher values at the centerline. Saetran and Byggstoyl (1985) used HW measurements to determine a centerline dissipation value (in similarity form) of 0.246, and Hussein et al. (1993) obtained a value of 0.32 using direct measurement. Based on these results and the earlier discussions, the present authors have concluded that there is not an off-axis peak, and rather arbitrarily assumed that the centerline dissipation value is somewhere near 0.26. A curve was then created that blends into the LDA data near $\eta = 0.10$. This curve is shown as the assumed profile in Figure 1. This is admittedly less than ideal, but is the best that can be done until accurate measurements are made.

Given the importance of the dissipation, it is prudent to determine how the present results would be affected if the true dissipation profile is different than the one assumed. To quantify this effect, the authors performed additional computations using the Model profile of Figure 1. With the exception of the pressure-transport term, this different dissipation profile did not significantly affect the results. The experimental values of the pressure-transport term were reduced by approximately 30 percent, with the model values

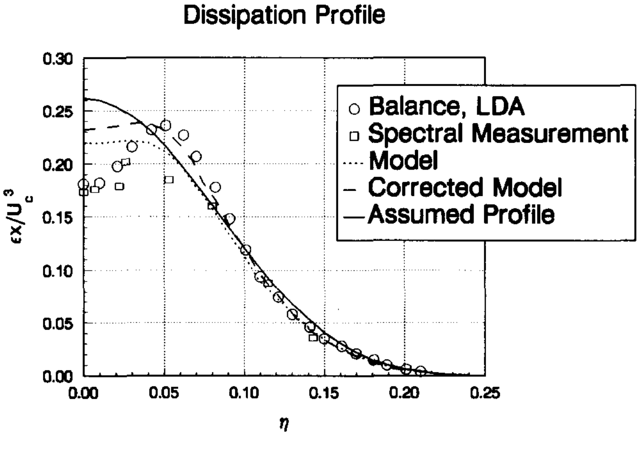

Figure 1 Dissipation profile

unaffected. The change to both the experimental and the model values for the pressure-strain correlations were small; less than 10 percent near the centerline, and less than 5 percent at the peak. The change to the model values of the transport correlations was negligible (on the order of 2 percent at the peak), with the experimental values unaffected. Based on these computations, use of a dissipation profile different than the one assumed for the present work would change the exact values of the results, but would not change the conclusions.

It should be noted that Hussein et al. (1993) performed an analysis of the jet data using a dissipation that was based on the assumption of local axisymmetry, as opposed to the more commonly used assumption of local isotropy, and obtained somewhat different results than those reported here. George and Hussein (1991) showed that the experimental data are more consistent with the assumption of local axisymmetry than the assumption of local isotropy. The axisymmetry assumption leads to a significantly larger dissipation than the isotrophic assumption, particularly near the centerline. It is unknown whether the dissipation is, in fact, as large as indicated by the axisymmetric assumption, or whether this higher calculated dissipation is due to some anomaly, such as the unmeasured derivatives being inconsistent with the axisymmetric assumption. The results obtained by these authors are interesting and warrant further study. It should also be noted that the dissipation is assumed to be isotropic in the development of turbulence models, and this is reflected in the values of the model coefficients. In accordance with this fact, computations by the present authors showed that the present assumed dissipation is in closer agreement with the turbulence models than the axisymmetric dissipation.

Reynolds stress models

The dynamic equation for the Reynolds stress for high Reynolds number flows can be written in Cartesian form as

$$\frac{D\overline{u_i u_j}}{Dt} = -\frac{\partial}{\partial x_k}(\overline{u_i u_j u_k} + \delta_{ik}\overline{pu_j}/\rho + \delta_{jk}\overline{pu_i}/\rho)$$
$$-\overline{u_i u_k}\frac{\partial U_j}{\partial x_k} - \overline{u_j u_k}\frac{\partial U_i}{\partial x_k} + \phi_{ij} - 2/3\varepsilon\delta_{ij} \tag{2}$$

In Reynolds stress calculations, the terms that need to be modeled in this equation are the triple-velocity correlation (first term on the right-hand side), pressure-transport terms (second and third terms on the right-hand side), and the pressure-strain correlation ϕ_{ij}. As previously mentioned, the pressure-transport term has been modeled by Lumley (1978) as $\overline{pu_i}/\rho = -0.2\overline{u_i q^2}$.

The pressure-strain correlation ϕ_{ij} consists of two parts: the return-to-isotropy part and the rapid-strain part. This can be written as

$$\phi_{ij} = \phi_{ij,1} + \phi_{ij,2} \tag{3}$$

The return-to-isotropy part can be modeled as (Lumley, 1978)

$$\phi_{ij,1} = -C_1\frac{\varepsilon}{k}(\overline{u_i u_j} - \tfrac{2}{3}\delta_{ij}k) + \gamma\varepsilon(b_{ik}b_{kj} + \tfrac{2}{3}\mathrm{II}\delta_{ij})$$

where (4)

$$b_{ij} = \overline{u_i u_j}/q^2 - \delta_{ij}/3 \quad \mathrm{II} = -b_{ik}b_{ki}/2$$

Equation 4 is referred to as the linear return-to-isotropy model if the coefficient γ is zero. Various proposals have been made for these coefficients, and their correct value has been an area of debate. Launder, Reese, and Rodi (1975) use $\gamma = 0$ and set

C_1 to a constant value of 1.5. This works well in some homogeneous shear flows, but has been shown to be inconsistent with other flows. Choi and Lumley (1984) developed expressions for C_1 and γ based on experiments of homogeneous flows without mean velocity gradients:

$$C_1 = 1 + 0.5\rho^* F^{1/2}/(1 + GX^2)$$
$$\rho^* = [7.69/R_l^{1/2} + 73.7/R_l - (296 - 16.2(1 + X)^4)\mathrm{II}] \times \exp(-9.29/R_l^{1/2})$$
$$\gamma = (2C_1 - 2)G/\zeta$$

where (5)

$$\zeta = (\mathrm{III}/2)^{1/3} \quad \mathrm{III} = b_{ij}b_{jk}b_{ki}/3 \quad \eta = (-\mathrm{II}/3)^{1/2} \quad X = \zeta/\eta$$
$$F = 1 + 27\mathrm{III} + 9\mathrm{II} \quad G = -X^4 + 0.8X^6 \quad R_l = 4k^2/9\nu\varepsilon$$

The expressions in Equation 5 have been shown to be inconsistent with several shear flows (Taulbee 1987), since the experiments used to develop the expressions were all low-Reynolds-number experiments, whereas shear flows are generally at high Reynolds number. The authors (see Lasher 1990) modified Equation 5 by taking the functional form for ρ^* and refitting it to six return-to-isotropy experiments and four homogeneous shear flow experiments. These experiments represent a more complete range of Reynolds number than those used by Choi and Lumley. C_1 can be inferred directly from the return-to-isotropy experiments, but obtaining the value of C_1 from the shear flow experiments is problematic. A model must be used for the rapid part of the pressure-strain correlation, which will necessarily contaminate the inferred value of C_1. We have little choice, however, if we are to include higher Reynolds number experiments in the coefficient. The inferred values of C_1 were then fit to Choi and Lumley's function using least squares to determine values for the free coefficients. This produced an expression that is valid for both low and high Reynolds numbers, and has been shown to work well in both return-to-isotropy and homogeneous shear flow predictions. The resulting expression is given in Equation 6:

$$\rho^* = [9.5/R_l^{1/2} + 230/R_l - (167 - 10.8(1 + X)^4)\mathrm{II}] \times \exp(-10.2/R_l^{1/2}) \qquad (6)$$

A similar expression for the linear part (C_1) was developed by Lumley (1978):

$$C_1 = 1 + F/18 \exp(-7.77/\sqrt{R_l})[72/\sqrt{R_l} + 80.1 \times \ln(1 + 62.4(-\mathrm{II} + 2.3\mathrm{III}))] \qquad (7)$$

The authors repeated the process used to modify the nonlinear model described above, resulting in the following expression:

$$C_1 = 1 + F/18 \exp(-3.1/\sqrt{R_1}) \times [29.0 \ln(1 - 71.0(\mathrm{II} + 14.3\mathrm{III}))] \qquad (8)$$

The rapid part of the pressure-strain correlation can be modeled as

$$\phi_{ij,2} = -\frac{(C_2 + 8)}{11}(P_{ij} - \tfrac{2}{3}P\delta_{ij}) - \frac{(30C_2 - 2)}{55}k\left(\frac{\partial U_i}{\partial x_j} + \frac{\partial U_j}{\partial x_i}\right) - \frac{(8C_2 - 2)}{11}(D_{ij} - \tfrac{2}{3}P\delta_{ij}) + \tfrac{4}{5}kC_{2f}\frac{\partial U_p}{\partial x_q}(\delta_{pj}b_{qi}^2 + \delta_{pi}b_{qj}^2 - 3b_{pq}b_{ij} - b_{qj}b_{pi} - b_{qi}b_{pj}) \qquad (9)$$

where

$$P_{ij} = -\left(\overline{u_iu_k}\frac{\partial U_j}{\partial x_k} + \overline{u_ju_k}\frac{\partial U_i}{\partial x_k}\right)$$
$$D_{ij} = -\left(\overline{u_iu_k}\frac{\partial U_k}{\partial x_j} + \overline{u_ju_k}\frac{\partial U_k}{\partial x_i}\right)$$

Launder et al. use the linear part ($C_{2f} = 0$) of this expression with $C_2 = 0.4$. Shih and Lumley (1985) developed the form for the nonlinear term in Equation 9 and gave the following expressions for C_2 and C_{2f}:

$$C_2 = -\frac{2}{3}\left[1 - \frac{11}{10}(1 + 0.8F^{1/2})\right] \qquad C_{2f} = 1 - F^{1/2} \qquad (10)$$

Speziale, Sarkar, and Gatski (1991) followed a different approach, using dynamical systems theory to develop an expression for the entire pressure-strain correlation, which is given as

$$\phi_{ij} = -(C_1\epsilon + C_1^*P)b_{ij} + C_2\epsilon(b_{ik}b_{kj} - 1/3b_{mn}b_{mn}\delta_{ij}) + (C_3 - C_3^*\mathrm{II}^{1/2})kS_{ij} + C_4k(b_{ik}S_{jk} + b_{jk}S_{ik} - 2/3b_{mn}S_{mn}\delta_{ij}) + C_5k(b_{ik}W_{jk} + b_{jk}W_{ik})$$

where (11)

$$S_{ij} = 1/2(\partial U_i/\partial x_j + \partial U_j/\partial x_i) \quad W_{ij} = 1/2(\partial U_i/\partial x_j - \partial U_j/\partial x_i)$$
$$C_1 = 3.4,\ C_1^* = 1.80,\ C_2 = 4.2,\ C_3 = 4/5,\ C_3^* = 1.30,$$
$$C_4 = 1.25,\ C_5 = 0.40$$

Equation 11 can be written in the same form as Equations 3, 4, and 9, but with significantly different coefficients. The model is nonlinear in the return part, but linear ($C_{2f} = 0$) in the rapid part.

The triple-velocity correlation (first term on the right-hand side of Equation 2) has been modeled by Launder et al. as

$$\overline{u_iu_ju_k} = C_s\frac{k}{\varepsilon}G_{ijk}$$

where (12)

$$G_{ijk} = \overline{u_iu_l}\frac{\partial\overline{u_ju_k}}{\partial x_l} + \overline{u_ju_l}\frac{\partial\overline{u_iu_k}}{\partial x_l} + \overline{u_ku_l}\frac{\partial\overline{u_iu_j}}{\partial x_l}$$

Equation 12 was developed by simplifying the dynamic equations for the third moments using a quasi-Gaussian approximation. Launder et al. assign a value of 0.11 to the constant C_s, which was determined by matching the model solution to experimental data. Lumley (1978) made an expansion about a Gaussian state, resulting in the following expression, which can easily be solved for $\overline{u_iu_ju_k}$:

$$\overline{u_iu_ju_k} + \frac{C_1 - 2}{9C_1}(\overline{u_iq^2}\delta_{jk} + \overline{u_jq^2}\delta_{ik} + \overline{u_kq^2}\delta_{ij}) = -\frac{1}{3C_1}\frac{\overline{q^2}}{\varepsilon}G_{ijk} \qquad (13)$$

C_1 is the coefficient in the closure for the return-to-isotropy model, and thus no additional parameters are introduced.

Comparison of models to experimental data

A comparison of the pressure-transport model given by Lumley ($\overline{pu_i}/\rho = -0.2\overline{u_iq^2}$) is compared with experimental data in Figure 2. The experimental values for the radial pressure-transport term $\overline{pv}$ were determined by balancing the energy

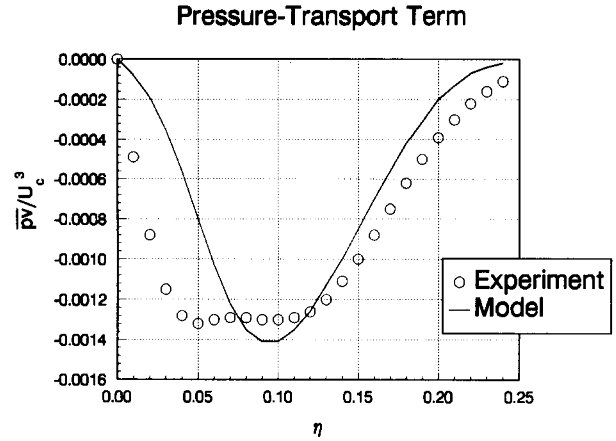

Figure 2 Pressure-transport term

equation. The axial transport term $\overline{pu}$ was estimated from Lumley's model, and the dissipation was the assumed profile in Figure 1. Any error in Lumley's estiamte for the axial transport term should have little effect on the results due to the relatively minor importance of that term. All other quantities were known, allowing determination of the radial transport term $\overline{pv}$.

Agreement between the model and experiment is reasonable. The model underpredicts the experimental values near the centerline, but the peak is well predicted. As discussed earlier, the experimental values are strongly affected by the assumed dissipation profile, especially near the centerline. This is because the slope of the pressure-transport curve is proportional to the dissipation. The close overall agreement between model and experiment is an indication that the value assumed for the centerline dissipation as discussed earlier is close to being correct.

The pressure-strain correlations were evaluated from Equation 2 using data from the LDA experiment for the mean flow and second and third moments; the assumed profile for the dissipation; Lumley's model for the axial pressure-transport term; and the experimental values shown in Figure 2 for the radial pressure-transport term. The experimental values are compared with the models given in Equations 3 to 11. Five different models are used; the nonlinear model uses the expression for ρ^* developed by the authors (Equation 6) in place of the ρ^* in Equation 5 to compute C_1 and γ, and by Shih and Lumley (1985) given in Equation 10 for C_2 and C_{2f}; the linear model uses the coefficient developed by the authors and given in Equation 8 for C_1 and the expression given in Equation 10 for C_2, with γ and $C_{2f} = 0$; the Launder et al. model is the linear model with $C_1 = 1.5$, $\gamma = 0$, $C_2 = 0.4$, and $C_{2f} = 0$; the Shih–Choi–Lumley model is Equation 5 for C_1 and γ, with Equation 10 for C_2 and C_{2f}; and the Speziale–Sarkar–Gatski (SSG) model is Equation 11. The equations and coefficients used for each model are summarized in Table 1.

Overall, the agreement between experiment and the models is good, as can be seen in Figures 3a–3d. None of the five models considered here demonstrates a clear superiority in predicting all four of the components; models that agree well with experiment for one component do not agree well for other

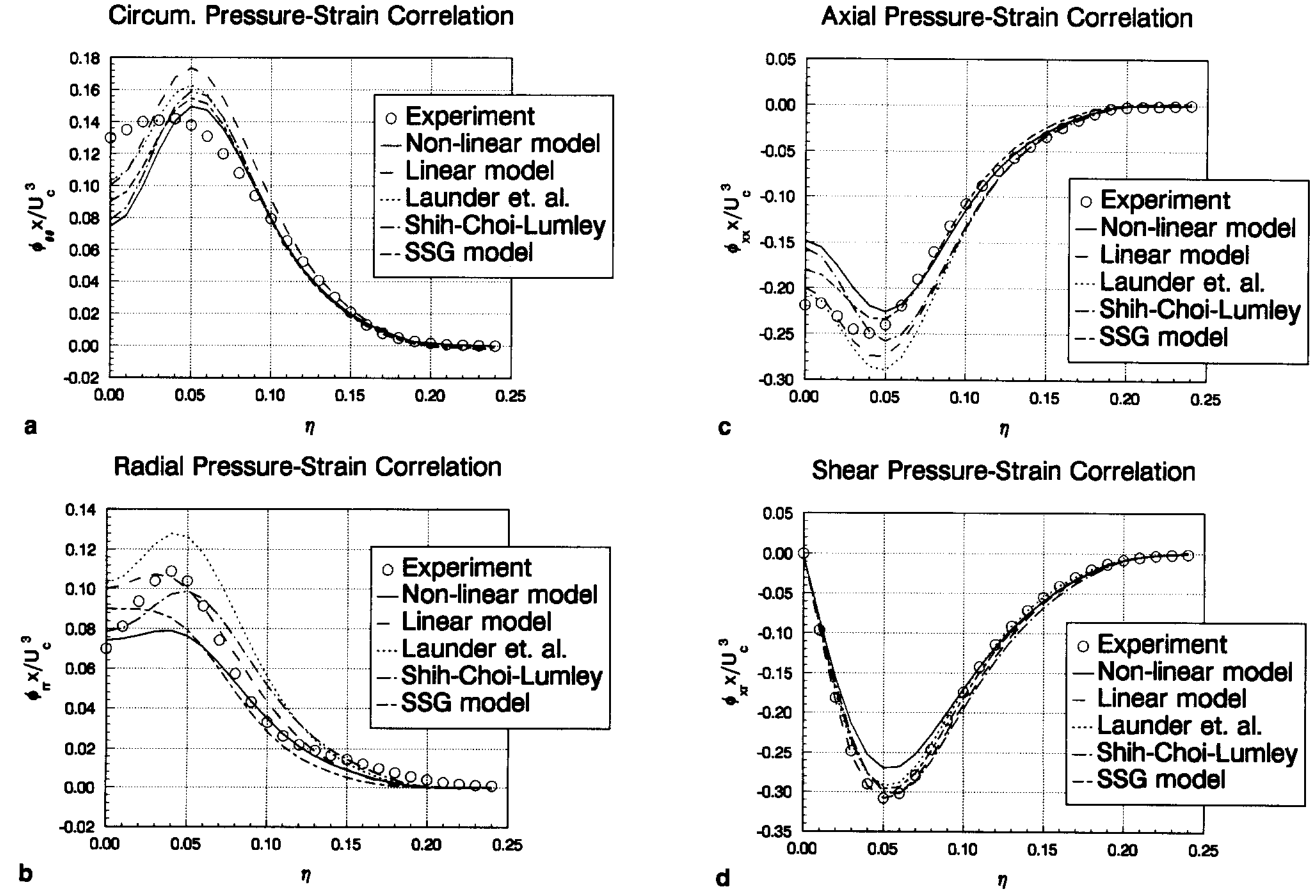

Figure 3 Pressure-strain correlation. (a) Circumferential correlation $\phi_{\theta\theta}$; (b) Radial correlation ϕ_{rr}; (c) Axial correlation ϕ_{xx}; (d) Shear correlation ϕ_{xr}

Table 1 Summary of equations and coefficients used for pressure-strain models

Model	C_1	γ	ρ^*	C_2	C_{2f}
Nonlinear	Eq. 5	Eq. 5	Eq. 6	Eq. 10	Eq. 10
Linear	Eq. 8	0	N/A	Eq. 10	0
Launder et al.	1.5	0	N/A	0.4	0
Shih–Choi–Lumley	Eq. 5	Eq. 5	Eq. 5	Eq. 10	Eq. 10
SSG	Equation 11				

components. In addition, a particular model may predict the peak value well but may not agree with experiment near the centerline, and vice versa.

It should be noted that agreement between the peak value of the model and experiment is probably a better indicator of success of the model than agreement between the centerline values. The experimentally inferred values have a higher level of uncertainty near the centerline than near the peaks for two reasons. First, we are not confident of the centerline value used for the dissipation. An increase or decrease in the centerline dissipation would improve agreement for one component and increase discrepancies for the others. Second, the slopes of the radial transport correlations are very difficult to measure accurately. These inaccuracies significantly influence the behavior of the experimentally inferred pressure-strain correlations near the centerline.

The present models (linear and nonlinear) are an improvement over both Launder's model and the Shih–Choi–Lumley model. One could not draw this conclusion on the basis of the present results alone, since the overall superiority of any of the models is insignificant. However, the present models are valid for both low-Reynolds-number return-to-isotropy flows and high-Reynolds-number shear flows, whereas the Launder et al. model has been shown to be incorrect for the return-to-isotropy flows, and the Shih–Choi–Lumley model has been shown to be incorrect for some other shear flows. Based on the present results, the nonlinear model is not superior to the linear model, which indicates that any possible advantages may not be worth the added computational complexity. Given its simplicity, the linear model is preferable for this flow. Work is currently in progress to further quantify the performance of the nonlinear model as compared to the linear model.

It should be noted that the SSG model, which predicts total pressure-strain components similar to the other models, predicts a significantly different decomposition into return-to-isotropy and rapid parts. Speziale, Gatski, and Sarkar (1992) argue that this decomposition is ambiguous for uniformly strained flows, and that what is important is the ability of the model to predict the total pressure-strain correlation. The latter point is certainly valid, and it is interesting that a model can predict such a different distribution into parts, yet agree with the total.

A comparison of the experimentally measured triple-velocity correlations with predictions from the models given by Launder et al. (Equation 12) and by Lumley (Equation 13) is shown in Figures 4a–4d. The coefficients used in the Lumley model is the present linear C_1 given in Equation 8, and is denoted as the present model in Figure 4. Agreement between the present model and experiment is good but erratic for the radial transport correlations (Figures 4a–4c). The prediction is

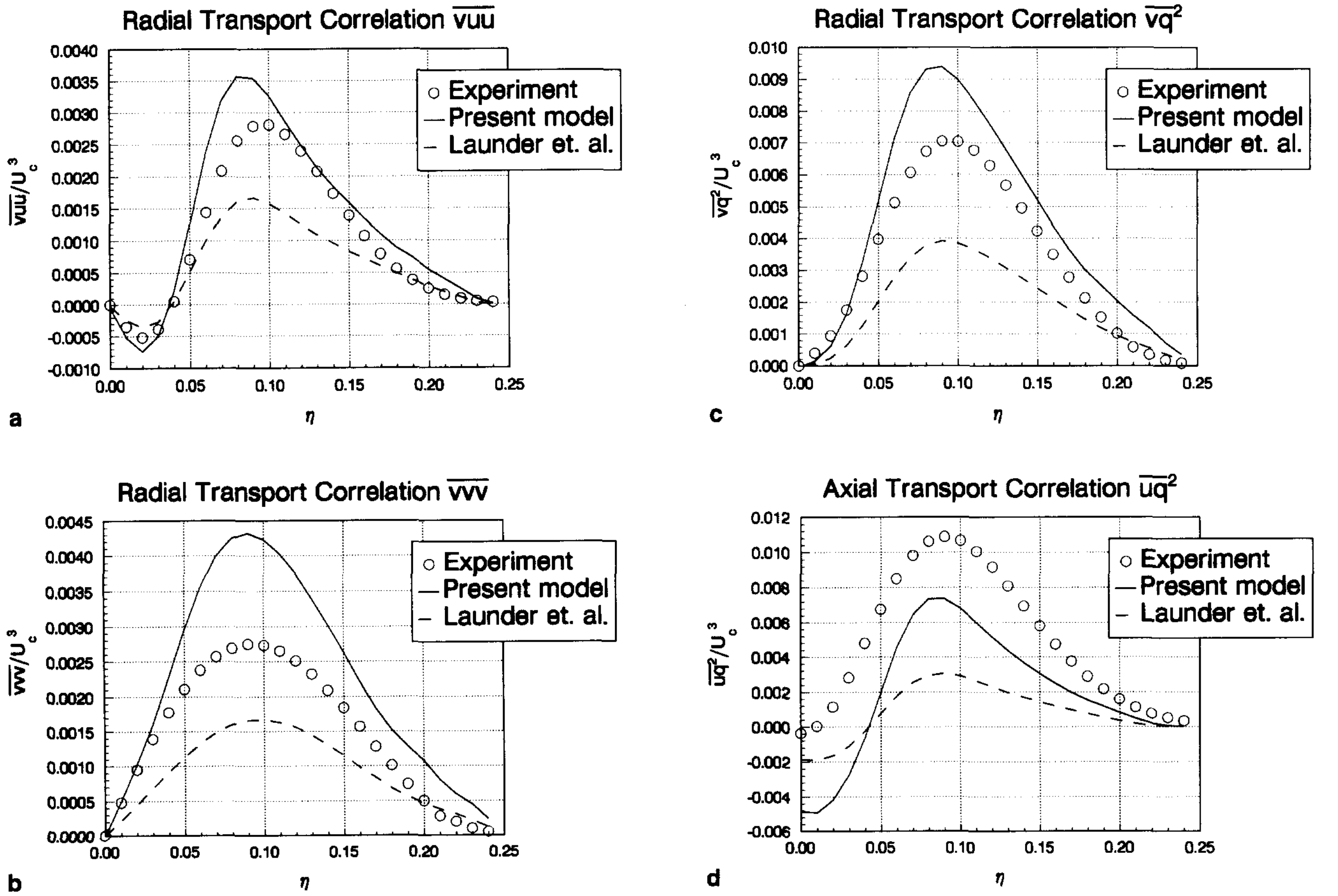

Figure 4 Transport correlation. (a) Radial correlation $\overline{vuu}$; (b) Radial correlation $\overline{vvv}$; (c) Radial correlation $\overline{vq^2}$; (d) Axial correlation $\overline{uq^2}$

excellent for the correlation $\overline{vuu}$, but significantly overpredicts the correlation $\overline{vvv}$. The model underpredicts the correlation $\overline{vww}$ (not shown), but it should be noted that this correlation was based on HW data as discussed earlier. The agreement with the correlation $\overline{vq^2}$ is also very good. On the whole, the present model is superior to the model given by Launder et al. It should be noted that the experimental data used by Launder et al. to tune their model contained the total effects of diffusion, including pressure diffusion, whereas in Lumley's model, pressure diffusion is explicit. This can explain a significant part of the difference between the Launder et al. model and experiment. Neither model accurately predicts the axial transport correlation $\overline{uq^2}$; however, this was not unexpected, since the gradient diffusion hypothesis is not really valid in the axial direction, where diffusion is relatively weak.

Schwarz and Bradshaw (1994) performed an analysis similar to the present work on a three-dimensional (3-D) boundary layer. There are several minor differences between their analysis and the present analysis, including their neglecting the pressure-transport term. They concluded that the models for the triple-velocity correlations are unrealistic and perform erratically. They state that some of this poor performance can be attributed to their neglecting pressure-transport; however, they estimate the pressure-transport term to be small. The better agreement between the present model and experiment in the present work is probably due in part to the pressure-transport term, and in part to the different coefficients used here. The comparison of the pressure-strain models to experimental data in the boundary layer is similar to that found here; specifically, the models predicted experiment well; there is little difference between the various model predictions; and the nonlinear models did not perform better than the linear model.

Summary

A comprehensive set of measurements from the turbulent axisymmetric jet given by Hussein et al. (1993) was used for evaluating single-point closure models. It has been shown that a complex flow in which the turbulence is governed by several distinct physical phenomena can be used for evaluating the individual components of a turbulence model. This approach has advantages over the commonly used approach, and requires only a few approximations.

The weaknesses of the present approach are that a model must be used for at least one component of the pressure-transport term, and the dissipation must be assumed to a certain extent. Due to the relatively minor importance of the pressure-transport term, the former weakness is probably not too important. Advances in experimental techniques will hopefully correct the latter weakness, possibly in the near future. In spite of these weaknesses, the present approach has provided valuable information.

The turbulence models that use the expressions for the return-to-isotropy coefficients developed by the authors have been shown to agree quite satisfactorily with the experimental data. Both the linear and nonlinear pressure-strain models agree reasonably well with the experimentally determined values. One would expect some discrepancy, considering the fact that the dissipation profile (which was assumed) affects the inferred value of the pressure-strain correlation. Agreement between the model and experiment for the triple-velocity correlations is good. It is certainly encouraging that models that were tuned to specific flows work so well in more complex flows.

References

Capp, S. P. 1983. Experimental investigation of the turbulent axisymmetric jet. Ph.D dissertation, State University of New York at Buffalo, NY

Choi, K. -S. and Lumley, J. L. 1984. Return to isotropy of homogeneous turbulence revisited. *Turb. Chaot. Phenomena Fluids*, T. Tatsume (ed.). Elsevier, North Holland, 267–272

George, W. K. and Hussein, H. J. 1991. Locally axisymmetric turbulence. *J. Fluid Mech.*, **233**, 1–23

Hanjalic, K. and Launder, B. E. 1980. Sensitizing the dissipation equations to irrotational strains. *J. Fluids Eng.*, **102**, 34–40

Hussein, H. J. 1988. Measurements of small scale turbulence in an axisymmetric jet using moving hot wires. Ph.D dissertation, Mechanical and Aerospace Engineering Dept., State University of New York at Buffalo, NY

Hussein, H. J., Capp, S. H., and George, W. K. In press. Velocity measurements in a high Reynolds number, momentum-conserving, axisymmetric, turbulent jet. *J. Fluid Mech.*

Lasher, W. C. 1990. The computation of complex, two-dimensional turbulent flows using Reynolds stress closure. Ph.D dissertation, Mechanical and Aerospace Engineering Dept., State University of New York at Buffalo, NY

Launder, B. E., Morse, A. P., Rodi, W., and Spaulding, D. B. 1973. The prediction of free-shear flows—a comparison of the performance of six turbulence models. *Proc. Langley Free-Shear Flows Conf.*, **1**, NASA SP320, Hampton, VA

Launder, B. E., Reece, G. J., and Rodi, W. 1975. Progress in the development of a Reynolds-stress turbulence closure. *J. Fluid Mech.*, **68**, 537–560

Lumley, J. L. 1978. Computational modeling of turbulent flows. *Adv. Appl. Mech.*, **18**, 123–176

Lumley, J. L. 1985. Interpretation of time spectra measured in high intensity shear flows. *Phys. Fluids*, **8**, 1056–1062

Pope, S. B. 1977. An explanation of the turbulent round jet/plane jet anomaly. Report No. FS/77/12, Imperial College, London, UK

Saetran, L. R. and Byggstoyl, S. 1985. Measurements of scalar dissipation along the centerline of a circular turbulent jet. *Proc. Fifth Symp. Turbulent Shear Flows*, Cornell University, Ithaca, NY

Schwarz, W. R. and Bradshaw, P. 1994. Term-by-term tests of stress-transport turbulence models in a three-dimensional boundary layer. *Phys. Fluids*, **6**, 986–998

Shih, T. -H. and Lumley, J. L. 1985. Modeling of pressure correlation terms in Reynolds stress and scalar flux equations. Mech. and Aero. Eng. Report FDA-85-3. Cornell University, Ithaca, NY

Specialize, C. G., Gatski, T. B. and Sarkar, S. 1992. On testing models for the pressure-strain correlation of turbulence using direct simulations. *Phys. Fluids*, **4**, 2887–2899

Speziale, C. G., Sarkar, S., and Gatski, T. B. 1991. Modeling the pressure-strain correlation of turbulence—an invariant dynamical systems approach. *J. Fluid Mech.*, **227**, 245–272

Taulbee, D. B. 1987. Engineering turbulence models. *Adv. Turbulence*, W. K. George, R. Arndt (eds). Hemisphere, New York, 75–125

Tennekes, H. and Lumley, J. L. 1972. *A First Course in Turbulence.* MIT Press, Cambridge, MA